Biosensors and Bioelectronics 24 (2009) 2285–2288

Contents lists available at ScienceDirect

Biosensors and Bioelectronics

journal homepage: www.elsevier.com/locate/bios

Short communication

# Electrochemical biosensing of methyl parathion pesticide based on acetylcholinesterase immobilized onto Au–polypyrrole interlaced network-like nanocomposite

Jingming Gong*, Lianyi Wang, Lizhi Zhang*

*Key Laboratory of Pesticide & Chemical Biology of Ministry of Education, College of Chemistry, Central China Normal University, Wuhan 430079, PR China*

ARTICLE INFO

*Article history:*
Received 11 October 2008
Received in revised form 8 November 2008
Accepted 11 November 2008
Available online 25 November 2008

*Keywords:*
Polypyrrole nanowires
Gold nanopaticles
Acetylcholinesterase
Methyl parathion
Biosensor

ABSTRACT

We developed a simple strategy for designing a highly sensitive electrochemical biosensor for organophosphate pesticides (OPs) based on acetylcholinesterase (AChE) immobilized onto Au nanoparticles–polypyrrole nanowires composite film modifid glassy carbon electrode (labeled as AChE–Au–PPy/GCE). Where, the generated Au nanoparticles (AuNPs) were homogenously distributed onto the interlaced PPy nanowires (PPy NWs) matrix, constructing a three-dimensional porous network. This network-like nanocomposite not only provided a biocompatible microenvironment to keep the bioactivity of AChE, but also exhibited a strong synergetic effect on improving the sensing properties of OPs. The combination of AuNPs and PPyNWs greatly catalyzed the oxidation of the enzymatically generated thiocholine product, thus increasing the detection sensitivity. On the basis of the inhibition of OPs on the enzymatic activity of AChE, the conditions for OPs detection were optimized by using methyl parathion as a model OP compound. The inhibition of methyl parathion was proportional to its concentration ranging from 0.005 to 0.12 and 0.5 to 4.5 $\mu g\,mL^{-1}$. The detection limit was 2 $ng\,mL^{-1}$. The developed biosensor exhibited good reproducibility and acceptable stability. This study provides a new promise tool for analysis of organophosphate pesticides.



## 1. Introduction

Because of the high toxicity, the extensive use of organophosphorous pesticides (OPs) for pest control has raised serious public concern regarding the healthiness, environment and food safety (Arduini et al., 2006; Li et al., 2007). OP compounds exhibit acute toxicity and irreversibly inhibit acetylcholinesterase (AChE), which often causes respiratory paralysis and death (Kim et al., 2005). Therefore, rapid determination and reliable quantification of trace level of OP compounds have become increasingly important for homeland security and health protection. Traditional analytical methods, such as gas or liquid chromatorgraphy and mass spectroscopy have been widely used for the determination of OPs (Chen and Huang, 2006; Rotiroti et al., 2005; Leandro et al., 2006). These methods, however, require complicated pretreatment steps, extensive labor resources, and are not applicable for on-site pesticides determination. Enzyme-based electrochemical biosensors have emerged the past few years as the most promising alternative to detect pesticides (Vakurov et al., 2004; Sotiropoulou et al., 2005; Jeanty and Marty, 1998; Sadik et al., 2003). Among them, electrochemical acetylcholinesterase (AChE) biosensors based on the inhibition on AChE have shown satisfactory results for pesticides analysis (Schulze et al., 2003; Kok and Hasirci, 2004; Shi et al., 2006), where the enzyme activity was employed as an indicator of quantitative measurement of insecticides. When AChE is immobilized on the working electrode surface, its interactions with the substrate of acetylthiocholine (ATCl) produce the electroactive product of thiocholine. The inhibition on the enzyme system can be monitored by measuring the oxidation current of thiocholine.

Effective immobilization of enzyme to solid electrode surface still remains a great challenge for the fabrication of biosensor. General methods include direct physical adsorption onto a solid supporting matrix (Sotiropoulou and Chaniotakis, 2005), entrapment in different substrate materials (Jeanty et al., 2001; Gong and Lin, 2003), self-assembly into multilayer film (Liu and Lin, 2006) and covalent binding (Lin et al., 2004). A key consideration for immobilizing enzyme is how to retain its bioactivity.

Polypyrrole (PPy), a key member of organic conducting polymers, has been widely used as the enzyme-hosting matrix for biomolecules, due to its advantages of permitting a facile electronic charge flow through the polymer matrix, easy preparation, high conductivity and good stability (Cosnier et al., 1999; Retama et al., 2004; Njagi and Andreescu, 2007). In particular, because of its

* Corresponding authors. Tel.: +86 27 6786 7535.
*E-mail addresses:* jmgong@mail.ccnu.edu.cn (J. Gong), zhanglz@mail.ccnu.edu.cn (L. Zhang).

0956-5663/$ – see front matter © 2008 Elsevier B.V. All rights reserved.
doi:10.1016/j.bios.2008.11.012

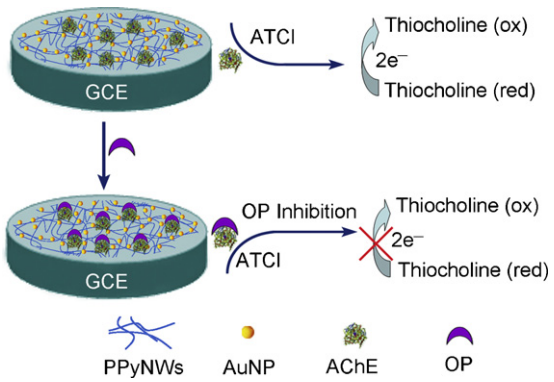


**Scheme 1.** Schematic illustration for biosensor fabrication and the principle of AChE used for determination of OP compound.

well-ordered polymer chain structure with high surface-to-volume ratio and small cross-dimensions, PPy nanowire has attracted considerable attention in the design of biosensors (Li and Lin, 2007). Recently, nanoparticles, especially the gold nanoparticles (AuNPs) have been extensively utilized in analytical electrochemistry (Sanz et al., 2005; Willner et al., 2006; Du et al., 2007), owing to their extraordinarily catalytic activities, good conductivity and biocompatibility.

Herein AuNPs and PPy nanowires are assembled together to act as an immobilization matrix of AChE. AuNPs are electrodeposited into the three-dimensional interlaced PPy nanowires network, leading to a stable and sensitive AChE sensor for rapid determination of methyl parathion (Scheme 1). Through the combination of PPy and AuNPs, this resulting composite matrix exhibits a porous structure with large effective surface areas, good conductivity and high catalytic activity, which greatly facilitates electron-transfer processes and the action of the immobilized AChE for OPs determination.

## 2. Experiments

### 2.1. Reagents

Pyrrole was obtained from Alfa Aesar and purified twice by distillation under the protection of high-purity nitrogen and then kept in a refrigerator before use. $HAuCl_4$ were purchased from Alfa Aesar. Acetylthiocholine chloride (ATCl) and AChE (Type C3389, 500 U $mg^{-1}$ from electric eel) were purchased from Sigma–Aldrich (St. Louis, USA) and used as received. Methyl parathion was obtained from Treechem Co. (Shanghai, China). All other chemicals were of analytical-reagent grade and used without further purification. Doubly distilled water and high-purity $N_2$ were used. The 0.1 mol $L^{-1}$ phosphate buffer solutions (PBS) of different pH values were prepared for the study. All experiments were carried out at ambient temperature.

### 2.2. Apparatus

Electrochemical measurements were performed on a CHI 660A electrochemical workstation (CHI, USA) with a conventional three-electrode system comprising platinum wire as auxiliary electrode, saturated calomel electrode (SCE) as reference and the modified or unmodified glass carbon electrode (GCE) as working electrode.

### 2.3. Electrode preparation

Prior to modification, the basal GCE was polished to a mirror finish using 1.0, 0.3 and 0.05 μm alumina slurries. After each polishing, the electrode was sonicated in ethanol and doubly distilled water for 5 min, successively, in order to remove any adsorbed substances on the electrode surface. Finally, it was dried under nitrogen atmosphere ready for use. PPy nanowires were fabricated according to the previous work (Tian et al., 2005). Typically, the PPy was electrochemically deposited at a constant potential of 0.80 V for 120 s in an aqueous solution of 0.1 mol $L^{-1}$ $LiClO_4$ and 0.1 mol $L^{-1}$ carbonate containing 0.15 mol $L^{-1}$ pyrrole. The electrode was then transferred into 0.1 mol $L^{-1}$ $HClO_4$ solution for 12 h aging. Thus the PPy nanowires modified electrode was obtained (denoted as PPy/GCE). The modification of AuNPs onto PPy/GCE was conducted by CV scanning from 0.2 to −1.0 V in 0.1 mol $L^{-1}$ KCl solution containing 0.5 mmol $L^{-1}$ $HAuCl_4$ at a scan rate of 50 $mVs^{-1}$ for 10 cycles (labeled as Au–PPy/GCE). After being thoroughly washed with double-distilled water, Au–PPy/GCE was further coated with 6 μL of AChE solution and incubated at 25 °C for 0.5 h to obtain the AChE–Au–PPy/GCE. This prepared sensor was stored at 4 °C for further use.

### 2.4. Measurement procedure

For the measurements of methyl parathion, the obtained AChE–Au–PPy/GCE was first immersed in PBS solution containing different concentrations of standard methyl parathion for 12 min, and then transferred to the electrochemical cell of 1.0 mL pH 7.0 PBS containing 1.0 mmol $L^{-1}$ ATCl to study the electrochemical response by cyclic voltammetry (CV). When the concentration of ATCl was too low, the peak current generated by enzyme electrode was so small that the determination of methyl parathion is hardly feasible. However, too high substrate concentration would cause all active centers of AChE being occupied by the substrate and insensible to the inhibitor. The concentration of 1.0 mmol $L^{-1}$ ATCl is an optimized value. The oxidation response of ATCl reached a plateau till its concentration increased to 1.0 mmol $L^{-1}$ at AChE–Au–PPy/GCE. The inhibition of methyl parathion was calculated as follows:

$$\text{inhibition } (\%) = \frac{i_{P,\text{control}} - i_{P,\text{exp}}}{i_{P,\text{control}}} \times 100$$

where $i_{P,\text{control}}$ is the peak current of ATCl on the AChE–Au–PPy/GCE, and $i_{P,\text{exp}}$ is the peak current of ATCl on the AChE–Au–PPy/GCE with methyl parathion inhibition.

## 3. Results and discussion

### 3.1. Characterization of electrode surface

The representative SEM images of the synthesized PPy nanowires and the Au–PPy nanocomposite onto GCE are shown in Fig. S1a and S1b, respectively. It can be seen that the sponge-like nanomatrix of PPy nanowires were formed onto the substrate (GCE) with ~60 nm in diameter (Fig. S1a). These PPy nanowires knotted with each other and interlaced together. As shown in Fig. S1b, with the successive deposition onto PPy/GCE, uniform AuNPs of ~20 nm in average diameter were decorated onto the surface and aligned along the PPy nanowires. Obviously, the generated AuNPs were homogenously distributed in the interlaced PPy nanowires matrix, constructing a three-dimensional interlaced porous network. As the supporting matrix, this porous composite film of Au–PPy provides a biocompatible and advantageous platform for biosensing applications.

### 3.2. Electrochemical behavior of AChE–Au–PPy/GCE

Fig. 1A shows the typical CVs of ATCl at 50 mV/s in 0.1 mol $L^{-1}$ pH 7.4 PBS. No peak was observed at bare GC electrode (curve a),

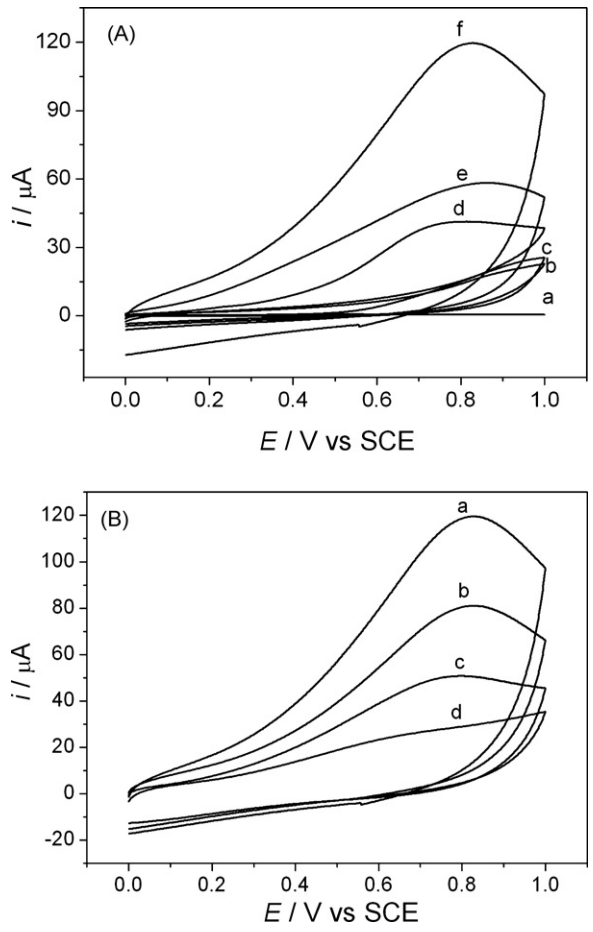


**Fig. 1.** (A) Cyclic voltammograms of (a) GCE; (b) AChE–Au–PPy/GCE in pH 7.0 PBS; (c) Au–PPy/GCE, (d) AChE–Au/GCE, (e) AChE–PPy/GCE, and (f) AChE–Au–PPy/GCE in pH 7.0 PBS containing 1.0 mM ATCl. Scan rate: 50 mV/s. (B) Cyclic voltammograms of AChE–Au–PPy/GCE in pH 7.0 PBS containing 1 mM ATCl after incubation in (a) 0, (b) 0.12, (c) 0.65 and (d) 2.5 μg mL$^{-1}$ methyl parathion solution, respectively, for 12 min.

and AChE–Au–PPy/GCE (curve b) in pH 7.0 PBS. When 1 mmol L$^{-1}$ ATCl was added into PBS, the CV of AChE–Au–PPy/GCE showed an obvious oxidation peak at 0.796 V (curve f), while no detectable signal was observed at Au–PPy/GCE (curve c). Obviously, this peak was attributed to the oxidation of thiocholine, hydrolysis product of ATCl, catalyzed by the immobilized AChE. Compared with the oxidation peak current of ATCl at AChE-PPy/GCE (curve e), one can see that the electrochemical response at AChE–Au–PPy/GCE was dramatically enhanced, with the oxidation overpotential reduced by 35 mV. This could be attributed to the presence of AuNPs in the nanocomposite film. These AuNPs with inherent conductive properties and catalytic behavior effectively promote the oxidation of the enzymatically generated thiocholine at a lower potential. If AuNPs were directly coated on the GCE electrode surface instead of entrapment in PPy nanowires network, only a small oxidation peak observed at AChE-Au/GCE (curve d). For comparison, chemically synthesized gold polypyrrole nanocomposite onto GCE (cAu–PPy/GCE) was also fabricated according to the literature procedure (Njagi and Andreescu, 2007). Compared with the oxidation response of ATCl at AChE-cAu–PPy/GCE, the oxidation peak potential at AChE–Au–PPy/GCE shifted negatively ~90 mV and the peak current was greatly enhanced (data not shown here). Obviously, the presence of Au–polypyrrole nanowires interlaced network-like nanocomposite film plays a great role. The generated AuNPs were homogenously distributed in the interlaced PPy nanowires matrix, constructing a three-dimensional interlaced porous network. It provides an advantageous and high-performance immobilization platform for enzyme (AChE). Furthermore, it greatly prompts the electron transport and shows more sensitive response than those modified by Au NPs or PPy NWs alone, exhibiting a strong synergetic effect on improving the sensing properties.

### 3.3. Effect of methyl parathion on response of AChE–Au–PPy/GCE

The produced current is related with the activity of immobilized enzyme, which can be used as an indicator for quantitative measurement of OPs. As shown in Fig. 1B, upon AChE–Au–PPy/GCE immersed in the standard solution of methyl parathion at a known concentration for 12 min, notably, the produced current decreased drastically (curves b–d). Moreover, the decrease in peak current increased with the further addition of methyl parathion. This was because methyl parathion as one of the OP pesticides exhibited fairly high acute toxicity and involved in the irreversible inhibition action on AChE, thus reduced the enzymatic activity to the pesticide substrate. Due to the notable change in voltammetric signal of the AChE–Au–PPy/GCE, the simple method for determination of methyl parathion could be established.

### 3.4. Effects of pH, inhibition time and temperature on the response of AChE–Au–PPy/GCE

The bioactivity of the immobilized AChE depended on the solution pH. Fig. S2a shows the relation between the peak current of ATCl and solution pH. Obviously, the maximum peak current was obtained at pH 7.0 in the pH range from 4.0 to 10.0. Therefore, pH 7.0 was used in the detection solution.

Inhibition time is one of the most influential parameters in pesticide analysis. With an increase of immersion time in the methyl parathion solution, the peak current of ATCl on the AChE–Au–PPy/GCE was decreased greatly. As shown in Fig. S2b, methyl parathion displayed an increasing inhibition on AChE with the immersion time increased. When the immersion time was longer than 12 min, the curve tended to a stable value, indicating the binding interactions with active target groups in the enzyme reached saturation. This change tendency of the peak current reflects an alteration of enzymatic activity, in turn resulting in the change of the interactions with its substrate. However, the maximum value of inhibition of methyl parathion was not 100%, which might be attributed to the binding equilibrium between pesticide and binding sites in the enzyme.

The effect of temperature on the response of the AChE–Au–PPy/GCE was observed. Fig. S2c shows the relationship between the temperature and the response of ATCl at AChE–Au–PPy/GCE in pH 7.0 PBS. During the temperature interval of 0–20 °C, the peak current of ATCl increased at AChE–Au–PPy/GCE, indicating an increased activity of the immobilized enzyme. Whereas, with the temperature increased from 20 to 50 °C, no obvious decrease in response was observed, indicating that the immobilized enzyme retained its activity well in the matrix. Obviously, the three-dimensional interlaced Au–PPy nanowires network provided a favorable microenvironment to maintain the bioactivity of AChE. For practical convenience, 25 °C was therefore selected as the operational temperature of the sensor.

### 3.5. Detection of methyl parathion

With increasing the concentration of methyl parathion in the immersion solution, the produced current of ATCl on the AChE–Au–PPy/GCE decreased. Under the optimized experimental conditions, the methyl parathion inhibition to AChE–Au–PPy/GCE was proportional to its concentration in two ranges, from 0.005 to 0.12 μg mL$^{-1}$ and 0.5 to 4.5 μg mL$^{-1}$. The linearization equa-

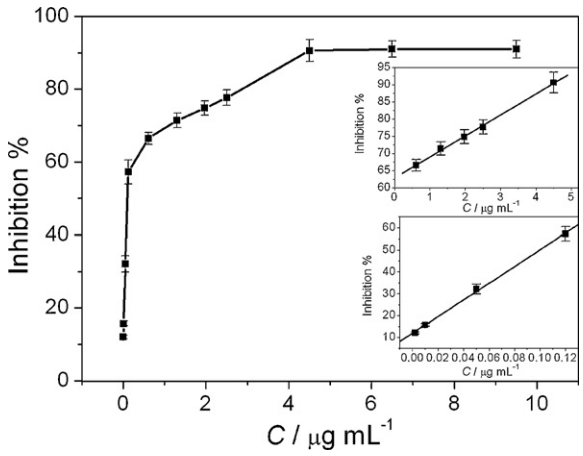


**Fig. 2.** Calibration curve for methyl parathion determination. (Inset) Linear relationships between peak currents and methyl parathion concentrations.

tions were inhibition (%) = 11.93$c$ + 381.44 (%), and inhibition (%) = 62.92$c$ + 6.11 (%), with the correlation coefficients of 0.9992 and 0.9989, respectively (Fig. 2). The detection limit was calculated to be about 2 ng mL$^{-1}$. The detection limit obtained is comparable with that reported so far with an enzyme-based inhibitor electrochemical sensor (Suprun et al., 2005), and it is significantly lower than those of 13.2 ng mL$^{-1}$ at carbon paste electrode by using stripping analysis (Liu and Lin, 2005), and also lower than 4.8 ng mL$^{-1}$ at the hanging mercury drop electrode (Ni et al., 2004), indicating that the proposed Au–PPy nanocomposite film is reliable for the determination of OP pesticides.

### 3.6. Precision, reproducibility and stability of AChE–Au–PPy/GCE

The intra-assay precision of the biosensors was evaluated by assaying one enzyme electrode for eight replicate determinations in 1.0 mmol L$^{-1}$ ATCl after being immersed in the 2.5 mol L$^{-1}$ methyl parathion solution for 12 min. Similarly, the inter-assay precision or fabrication reproducibility, was estimated at eight different electrodes. The R.S.D. of intra-assay and inter-assay were found to be 5.0% and 8.4%, respectively, indicating acceptable reproducibility.

The stability of the enzyme electrode could be maintained by being stored at 4 °C in dry condition. No obvious decrease in the response of ATCl was observed in the first 10-day storage. After a 30-day storage period, the sensor retained 60% of its initial current response. The responses of the sensors have decreased with the number of measurements. The interferences from the other electroactive nitrophenyl derivatives such as nitrobenzene, nitrophenol and other oxygen-containing inorganic ions ($PO_4^{3-}$, $SO_4^{2-}$, $NO_3^-$) were investigatd. No obvious inhibition behavior can be observed with the peak currents of ATCl varied slightly.

### 3.7. Reactivation of AChE–Au–PPy/GCE

The AChE inhibited irreversibly by OPs can be completely reactivated by use of nucleophilic compounds such as pralidoxime iodide. It was observed that AChE modified electrode inhibited by methyl parathion could resume 95% original activity after immersing in 5.0 mM pralidoxime iodide (Fig. S3a). With increasing reactivation time, the reactivation efficiency $R$% increased and reached stable at ~10 min (Fig. S3b). Based on this reactivation procedure, the proposed biosensor could be used repeatedly with an acceptable reproducibility.

## 4. Conclusions

This work demonstrated a simple and efficient strategy for immobilization of AChE, as a model enzyme, onto the composite film of Au–PPy/GCE. As an immobilization matrix of AChE, the three-dimensional interlaced PPy nanowires network provided a favorable microenvironment to maintain the bioactivity of AChE. Meanwhile, AuNPs distributed in the network-structured PPy matrix greatly facilitated electron transfer, leading to a stable and sensitive AChE sensor for rapid determination of OPs. The resulting biosensor showed good precision, reproducibility, and stability. We believe that this nanocomposite film will pave the way to the new AChE-based inhibitor biosensor for OPs determination. Such a hybrid biocompatible film will be attractive to construct other enzyme-based inhibitor biosensor to detect toxic compounds.

## Acknowledgements

This work was supported by National Basic Research Program of China (973 Program) (Grant 2007CB613301), National Science Foundation of China (Grants 20803026, 20503009, 20673041 and 20777026), Program for New Century Excellent Talents in University (Grant NCET-07-0352), and the Key Project of Ministry of Education of China (Grant 108097).

## Appendix A. Supplementary data

Supplementary data associated with this article can be found, in the online version, at doi:10.1016/j.bios.2008.11.012.

## References

Arduini, F., Ricci, F., Tuta, C.S., Moscone, D., Amine, A., Palleschi, G., 2006. Anal. Chim. Acta 580, 155–162.
Chen, P.S., Huang, S.D., 2006. Talanta 69, 669–675.
Cosnier, S., Senillou, A., Gratzel, M., Comte, P., Vlachopoulos, N., Renault, N.J., Mertelet, C., 1999. J. Electroanal. Chem. 469, 176–181.
Du, D., Chen, S.Z., Cai, J., Zhang, A.D., 2007. Biosens. Bioelectron. 23, 130–134.
Gong, J.M., Lin, X.Q., 2003. Microchem. J. 75, 51–57.
Jeanty, G., Ghommidh, Ch., Marty, J.L., 2001. Anal. Chim. Acta 436, 119–128.
Jeanty, G., Marty, J.L., 1998. Biosens. Bioelectron. 13, 213–218.
Kim, T.H., Kuca, K., Jun, D., Jung, Y.K., 2005. Bioorg. Med. Chem. Lett. 15, 2914–2917.
Kok, F.N., Hasirci, V., 2004. Biosens. Bioelectron. 19, 661–665.
Leandro, C.C., Hancock, P., Fussell, R.J., Keely, B.J., 2006. J. Chromatorgr. A 1103, 94–101.
Li, B.X., He, Y.Z., Xu, C.L., 2007. Talanta 72, 223–230.
Li, J., Lin, X.Q., 2007. Biosens. Bioelectron. 22, 2898–2905.
Lin, Y., Lu, F., Wang, J., 2004. Electroanalysis 16, 145–149.
Liu, G.D., Lin, Y.H., 2006. Anal. Chem. 78, 835–843.
Liu, G.D., Lin, Y.H., 2005. Electrochem. Commun. 7, 339–343.
Ni, Y.N., Qiu, P., Kokot, S., 2004. Anal. Chim. Acta 516, 7–17.
Njagi, J., Andreescu, S., 2007. Biosens. Bioelectron. 23, 168–175.
Retama, J.R., Cabarcos, E.L., Mecerreyes, D., Lopez-Ruiz, B., 2004. Biosens. Bioelectron. 20, 1111–1117.
Rotiroti, L., Stefano, L.D., Rendina, I., Moretti, L., 2005. Biosens. Bioelectron. 20, 2136–2139.
Sadik, O., Land, W., Wang, J., 2003. Electroanalysis 15, 1149–1159.
Sanz, V.C., Luz Mena, M., Gonzïalez-Cortïes, A., Yïanez-Sedeno, P., Pingarrïon, J.M., 2005. Anal. Chim. Acta 528, 1–8.
Schulze, H., Vorlovïa, S., Villatte, F., Bachmann, T.T., Schmid, R.D., 2003. Biosens. Bioelectron. 18, 201–209.
Shi, M., Xu, J.J., Zhang, S., Liu, B.H., Kong, J.L., 2006. Talanta 68, 1089–1095.
Sotiropoulou, S., Chaniotakis, N.A., 2005. Anl. Chim. Acta 530, 199–204.
Sotiropoulou, S., Fournier, D., Chaniotakis, N.A., 2005. Biosens. Bioelectron. 20, 2347–2352.
Suprun, E., Evtugyn, G., Budnikov, H., Picci, F., Moscone, D., Palleschi, G., 2005. Anal. Bioanal. Chem. 383, 597–604.
Tian, Y., Wang, J.X., Wang, Z., Wang, S.C., 2005. Sens. Actuator B 104, 23–28.
Vakurov, A., Simpson, C.E., Daly, C.L., Gibson, T.D., Millner, P.A., 2004. Biosens. Bioelectron. 20, 1118–1125.
Willner, I., Baron, R., Willner, B., 2006. Adv. Mater. 18, 1109–1120.